Side-Chain Engineering for High-Performance Conjugated Polymer Batteries

Xiaoyi Li, Yilin Li, Kasturi Sarang, Jodie Lutkenhaus,* and Rafael Verduzco*

Conjugated polymers are attractive for energy storage but typically require significant amounts of conductive additives to successfully operate with thin electrodes. Here, side-chain engineering is used to improve the electrochemical performance of conjugated polymer electrodes. Naphthalene dicarboximide (NDI)-based conjugated polymers with ion-conducting ethylene glycol (EG) side chains (PNDI-T2EG) and non-ion-conducting 2-octyldodecyl side chains (PNDI-T2) are synthesized, tested, and compared. For thick (20 µm, 1.28 mg cm^{-2}) electrodes with a 60 wt% polymer, the PNDI-T2EG electrodes exhibit 66% of the theoretical capacity at an ultrafast charge–discharge rate of 100C (72 s per cycle), while the PNDI-T2 electrodes exhibit only 23% of the theoretical capacity. Electrochemical impedance spectroscopy measurements on thin (5 µm, 0.32 mg cm^{-2}), high-polymer-content (80 wt%) electrodes reveal that PNDI-T2EG exhibits much higher lithium-ion diffusivity ($D_{Li+} = 7.01 \times 10^{-12}$ cm^2 s^{-1}) than PNDI-T2 ($D_{Li+} = 3.96 \times 10^{-12}$ cm^2 s^{-1}). PNDI-T2EG outperforms most previously reported materials in thick, high-polymer-content electrodes in terms of rate performance. The results demonstrate that the rate performance and capacity are significantly improved through the incorporation of EG side chains, and this work demonstrates a route for increasing the rate of ion transport in conjugated polymers and improving the performance and capacity of conjugated-polymer-based electrodes.

1. Introduction

Organic electrode materials offer several advantages over inorganic materials. They are rich in carbon and hydrogen and do not contain heavy metals, resulting in materials that are relatively inexpensive to manufacture and that can be potentially recycled. They are soft and lightweight, enabling the incorporation into portable and flexible batteries.[1] They also do not require the high processing temperatures commonly required for processing inorganic electrode materials.[2,3] Therefore, they

are more favorable from an economic- and environmental-impact perspective. A broad range of organic electrode materials has been developed for energy storage,[4–7] including hydrocarbons,[8–10] amines,[11–13] thioethers, disulfides,[14–16] nitroxyl radicals,[17–19] and carbonyls.[20]

Conjugated polymers are attractive organic materials for energy storage. When electrochemically doped by cations (e.g., lithium ions, magnesium ions), these materials exhibit intrinsic electronic conductivity which can help transport charges[21,22] and enable operation at very high charge–discharge rates. Furthermore, conjugated polymer-based electrodes are more stable than small molecular-based electrodes due to limited or no solubility in the liquid electrolyte.[23] However, conjugated polymer electrodes (even small molecules) require significant amounts of conductive additives, typically 30–50 wt% of the electrode mass.[5–7] This is due to insufficient electronic conductivity. Furthermore, they generally exhibit poor lithium-ion conductivities, and, as a result, their storage capacities drop significantly with electrode thickness. The poor electronic and ionic conductivities significantly limit the practical application of conjugated polymers in batteries such as electronic devices and electric vehicles, where fast (i.e., charge in less than 30 min) or even ultrafast (i.e., charge in less than 5 min) rechargeability is more desirable than high capacities.

Here, we propose that these issues can be addressed in part through engineering the side chains of the conjugated polymers. While a variety of different conjugated polymer chemistries have been studied, these primarily focus on the composition of the backbone repeat unit rather than the side chain.[6,7] We hypothesized that the composition of the conjugated polymer side chain could impact polymer properties directly relevant to energy storage. This includes the solubility and processability of the material, the electronic and ionic conductivities in the conjugated polymer electrode, and the nature of electrochemical interactions between the lithium ions and the conjugated backbone.

Several recent studies have investigated the physical and chemical properties of conjugated polymers with polar side chains, which are examples of polymers with mixed ionic and electronic conduction.[24,25] The polar side chains can enhance compatibility with the dopants and improve processibility,[26]

Dr. X. Li, Dr. Y. Li, Prof. R. Verduzco
Department of Chemical and Biomolecular Engineering
Rice University
Houston, TX 77005, USA
E-mail: rafaelv@rice.edu
K. Sarang, Prof. J. Lutkenhaus
Department of Chemical Engineering
Texas A&M University
College Station, TX 77843, USA
E-mail: jodie.lutkenhaus@tamu.edu

2009263 (1 of 7)

**ADVANCED
SCIENCE NEWS**
www.advancedsciencenews.com

**ADVANCED
FUNCTIONAL
MATERIALS**
www.afm-journal.de

thermal stability,[27] and doping efficiency.[28] These types of polymers have also been implemented in several applications, including thermoelectrics,[29] n-type[30] and p-type[31,32] organic electrochemical transistors (OECTs), and electrochromic devices.[33] While the introduction of polar side chains can enhance performance for these applications, other studies have also pointed to trade-offs between electron mobility and capacitance with increased polar side-chain content[34] and disruption of favorable structural and electronic properties in some cases.[35]

In this work, we synthesized a naphthalene dicarboximide (NDI)-based polymer with ethylene glycol (EG) side chains (**PNDI-T2EG**), as shown in **Figure 1** (see Scheme S1 and Figures S1–S12 in the Supporting Information for synthetic details). As a comparison, a polymer with 2-octyldodecyl side chains (**PNDI-T2**) was also synthesized. Oligo- and poly-ethylene glycol-based materials have excellent lithium-ion conductivities and are commonly used as solid electrolytes to transport lithium-ion,[36,37] and we hypothesized that by covalently attaching EG side chains to the NDI backbone, we could improve the diffusivity of lithium ions in the polymer electrodes and enhance the doping of the conjugated backbone, enabling faster charge–discharge kinetics and better performance for both thicker and higher polymer content electrodes. **PNDI-T2EG** has been previously reported by Giovannitti et al. in the first demonstration of an n-type and ambipolar OECT.[30] The devices exhibited excellent stability in water with excellent peak current and transconductance. Other recent studies with NDI-based polymers have reported excellent performance of these materials in lithium-ion batteries, magnesium batteries, and redox flow batteries.[38–41] However these studies did not investigate the impact of side chains on redox activity or energy storage capacity of these materials in batteries. Our results presented below demonstrate that the rate performance, storage capacity, and performance with increasing electrode thickness and polymer content were significantly improved through the incorporation of EG side chains.
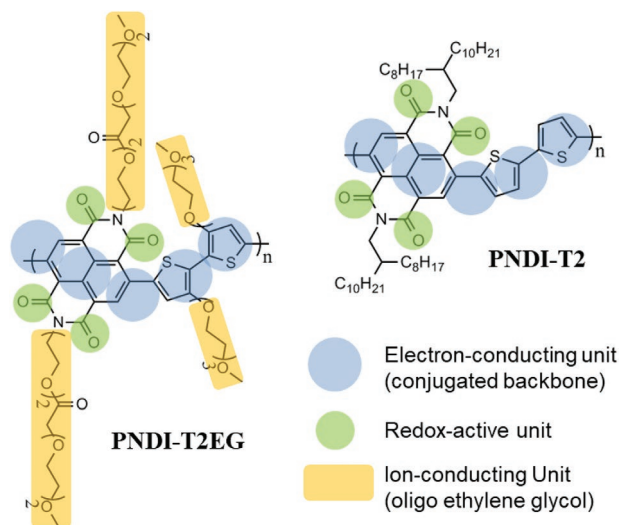
2. Results and Discussion

To test the electrochemical performance, we fabricated nanocomposite electrodes by blending the polymers with conductive carbon (Super-P). We first tested electrodes with 60 wt% polymer (balance was 40 wt% conductive carbon) at two different electrode mass loadings, 0.32 and 1.28 mg cm^{-2}, corresponding to thin ($\approx$5 µm) and thick ($\approx$20 µm) electrodes, respectively. Assuming a two-electron reaction with each NDI unit in the polymer,[42] the theoretical specific capacity was 54.2 mAh g^{-1} for **PNDI-T2** and 42.9 mAh g^{-1} for **PNDI-T2EG**. We normalized the capacities by the theoretical capacity, and the unnormalized specific capacities for the polymers are provided in the Supporting Information. The charge–discharge rate was represented by C-rate rather than current density, and Table S1 in the Supporting Information provides the relationship between C-rate, current density, and charge–discharge time for the electrodes studied. In this study, we systematically varied the C-rate from 1C (2 h per charge–discharge cycle) up to 500C (14.4 s per cycle). The experiments were performed on at least three identical electrodes and repeated at least three times to ensure the reproducibility of the results. We report the average of these three studies.

The measured specific capacities relative to the theoretical specific capacity for thin (5 µm, 0.32 mg cm^{-2}) **PNDI-T2EG** and **PNDI-T2** electrodes is shown in **Figure 2**a (see Table S2 in the Supporting Information for the unnormalized results). In terms of the normalized specific capacity, the **PNDI-T2EG** electrodes performed worse than the **PNDI-T2** electrodes up to 200C (36 s per cycle). For example, the **PNDI-T2EG** electrodes exhibited about 80% of the theoretical specific capacity at 20C (6 min per cycle), while the **PNDI-T2** electrodes exhibited nearly 100%. At 500C (14.4 per cycle), both polymer electrodes exhibited comparable normalized specific capacities. For the unnormalized specific capacity as shown in Table S2 (Supporting Information), the **PNDI-T2** electrodes exhibited higher values than the **PNDI-T2EG** electrodes over the entire measured range of C-rate. The only advantage of **PNDI-T2EG** over **PNDI-T2** in the thin (5 µm, 0.32 mg cm^{-2}) electrodes was that the **PDNI-T2EG** electrodes exhibited a slower decrease in the normalized specific capacity with increasing C-rate than the **PDNI-T2** electrodes, which suggested faster redox kinetics that allowed fast rechargeability through efficient electron and ion transport.

A much greater difference in normalized specific capacity was observed in thicker electrodes (20 µm, 1.28 mg cm^{-2}), as shown in Figure 2b (see Table S3 in the Supporting Information for the unnormalized results). First, the **PNDI-T2EG** electrodes exhibited higher normalized specific capacities than the **PDNI-T2** electrodes, especially at higher C-rates ($\geq$20C). For C-rates below 10C (12 min per cycle), the **PNDI-T2EG** electrodes exhibited comparable normalized specific capacities with those of the **PNDI-T2** electrodes, while for C-rates greater than 20C (6 min per cycle), the **PNDI-T2EG** electrodes exhibited higher normalized specific capacities than the **PNDI-T2** electrodes. Second, the **PNDI-T2** electrodes exhibited a significant drop in the normalized specific capacity with increasing C-rate, and the normalized specific capacity was zero at 200C (36 s per cycle) and 500C (14.4 s per cycle). Conversely, the
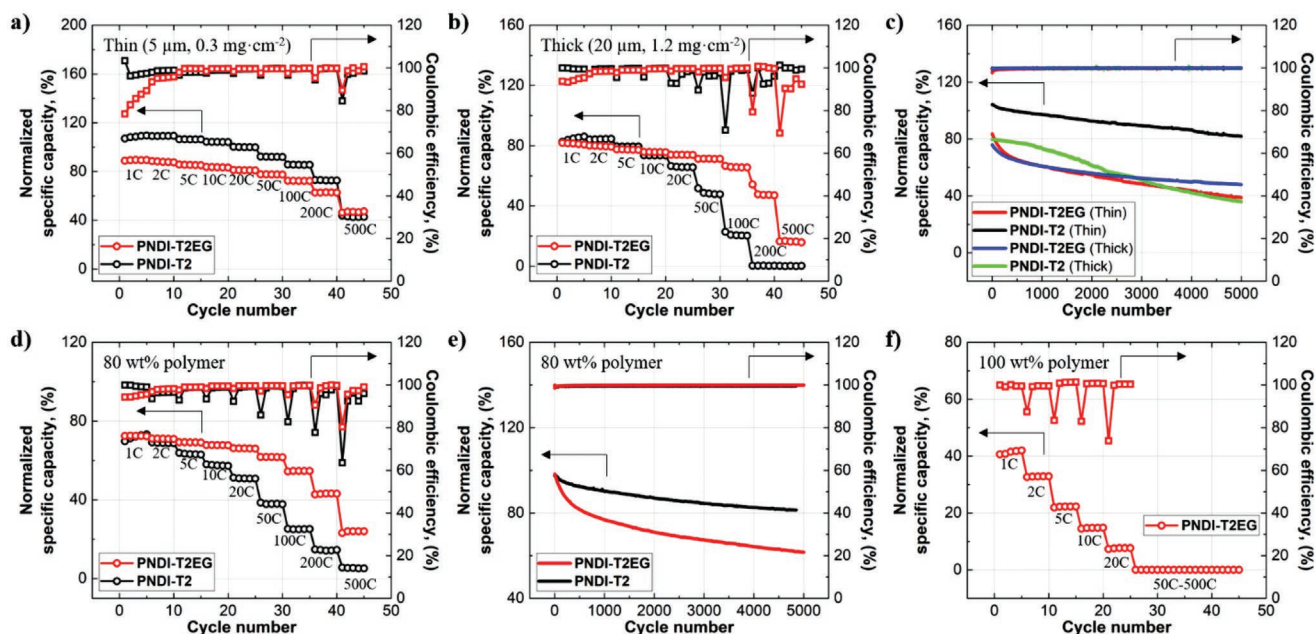

Figure 1. Chemical structures of **PNDI-T2** and **PNDI-T2EG** and the structural functionalities.

Figure 2. Normalized specific capacity (defined as the measured specific capacity relative to the theoretical specific capacity) and Coulombic efficiency with increasing C-rate for a) thin (5 μm, 0.32 mg cm^{-2}) and b) thick (20 μm, 1.28 mg cm^{-2}) **PNDI-T2EG** and **PNDI-T2** electrodes comprised of 60 wt% polymer (see Figures S13 and S14 in the Supporting Information for detailed charge–discharge curves). c) Normalized specific capacity and Coulombic efficiency with increasing cycle number for thin (5 μm, 0.32 mg cm^{-2}) and thick (20 μm, 1.28 mg cm^{-2}) **PNDI-T2EG** and **PNDI-T2** electrodes comprised of 60 wt% polymer. Normalized specific capacity and Coulombic efficiency with increasing d) C-rate and e) cycle number for thin (5 μm, 0.32 mg cm^{-2}) **PNDI-T2EG** and **PNDI-T2** electrodes comprised of 80 wt% polymer. f) Normalized specific capacity and Coulombic efficiency with increasing C-rate for thin (5 μm, 0.32 mg cm^{-2}) **PNDI-T2EG** electrodes comprised of 100 wt% polymer.

PNDI-T2EG electrodes were capable of sustaining 70% of the theoretical specific capacity at 100C (72 s per cycle), and the **PNDI-T2EG** electrodes still exhibited electrochemical performance at a C-rate of 500C (14.4 s per cycle). For the unnormalized specific capacity as shown in Table S3 (Supporting Information), the **PNDI-T2EG** electrodes exhibited higher specific capacities than the **PNDI-T2** electrodes at 50C (144 s per cycle) and higher charge–discharge rates. This reflects the faster redox kinetics for **PNDI-T2EG** over **PNDI-T2** in thick (20 μm, 1.28 mg cm^{-2}) electrodes.

We also investigated the cycling stability of the nanocomposite electrodes at both high and low mass loadings. Figure 2c shows long-term cycling studies (up to 5000 charge–discharge cycles) at a charge–discharge rate of 10C (12 min per cycle). For thin (5 μm, 0.32 mg cm^{-2}) electrodes, the **PNDI-T2** electrodes exhibited higher long-term stability with higher normalized specific capacities than the **PNDI-T2EG** electrodes. For the thick (20 μm, 1.28 mg cm^{-2}) electrodes, the **PNDI-T2EG** electrodes outperformed the **PNDI-T2** electrodes. The **PNDI-T2EG** electrodes exhibited 50% of the theoretical specific capacity after 5000 cycles, which was approximately 10% greater than the **PNDI-T2** electrodes.

We also tested the potential self-discharge of the thick (20 μm, 1.28 mg cm^{-2}) organic electrodes, which has been reported in some organic electrode materials.[43–45] To test this, we charged the batteries and then disconnected the batteries, and allowed them to rest for a fixed time (up to 14 days) before measuring the state-of-charge. As shown in Table S4 of the Supporting Information, batteries comprised of the **PNDI-T2**

and **PNDI-T2EG** electrodes were capable of sustaining over 97% of initial specific capacities for 14 days, which were superior to batteries comprised of other polymer electrodes which exhibited an approximate 1% daily decrease in the specific capacity.[43–45]

Next, we varied the content of conductive additives in the nanocomposite electrodes. Conductive additives such as Super P carbon are typically used in organic electrodes at 30–60 wt% as most organic materials are intrinsically nonconductive.[5,7,21,46] **PNDI-T2** and **PNDI-T2EG** are semiconducting polymers that become conductive after electrochemical doping, but conductive additives are still needed as their intrinsic conductivities are too low. The conductive additives do not directly contribute to the charge storage capacity of the electrodes, and therefore minimizing the content of conductive additives is desirable to increase the charge storage capacity of the electrodes.

To this end, we fabricated thin (5 μm, 0.32 mg cm^{-2}) **PNDI-T2** and **PNDI-T2EG** nanocomposite electrodes with 80 wt% polymer and repeated both rate performance and cycling stability. As shown in Figure 2d, the normalized specific capacity of the **PNDI-T2** electrodes decreased significantly with increasing C-rate over the entire range tested, while that of the **PNDI-T2EG** electrodes decreased only slightly for the C-rate less than 20C (6 min per cycle) (see Table S5 in the Supporting Information for the unnormalized results). The **PNDI-T2EG** electrodes at 100C (72 s per cycle) exhibited 60% of the theoretical specific capacities compared with just 20% for the **PNDI-T2** electrodes. For the unnormalized specific

**ADVANCED
SCIENCE NEWS**
www.advancedsciencenews.com

**ADVANCED
FUNCTIONAL
MATERIALS**
www.afm-journal.de

capacity as shown in Table S5 (Supporting Information), the **PNDI-T2EG** electrodes exhibited a higher specific capacity than the **PNDI-T2** electrodes at C-rates greater than 20C (6 min per cycle). Despite a poor rate performance, the cycling stability of the **PNDI-T2** electrodes was greater than that of the **PNDI-T2EG**, as shown in Figure 2e. This may be due to a much lower molecular weight of **PNDI-T2EG** (7.55 kg mol^{-1}) than that of **PNDI-T2** (108 kg mol^{-1}).

The superior rate performance of the **PNDI-T2EG** electrodes with 80 wt% polymer encouraged us to further increase the polymer content to 100 wt% (i.e., additive-free, pure polymer electrodes). Surprisingly, the **PNDI-T2EG** electrodes exhibited significant and measurable electrochemical performance up to 20C with near 100% Coulombic efficiency, while the **PNDI-T2** electrodes failed during electrochemical cycling measurements, as shown in Figure 2f. The absolute specific capacity of **PNDI-T2** electrodes was zero at all C-rates tested (not shown in the plot). The additive-free, pure **PNDI-T2EG** electrodes signified that the EG-side chains significantly improved the electronic conductivity of the electrodes in addition to the ionic conductivity. To the best of our knowledge, no similar additive-free organic electrode material has been reported. The ability for these polymers to function as pure polymer-based electrodes is attributed to doping of the conjugated backbone by lithium ions and is discussed below.

These results demonstrate the superior electrochemical performance of **PNDI-T2EG** compared against **PNDI-T2** and indicate a positive impact of the EG side chains on redox kinetics of the polymer electrodes. In practical conditions such as thick electrodes and high polymer content, **PNDI-T2EG** exhibited higher absolute specific capacities than **PNDI-T2** at fast charge–discharge conditions, both in terms of C-rate and current density (see Table S3 and Tables S5 and S6 in the Supporting Information). We attributed this to the improved ion diffusivity in the **PNDI-T2EG** electrodes imparted by the EG side chains. Electrochemical impedance spectroscopy (EIS) measurements provided direct evidence of the improved ion diffusivity in the **PNDI-T2EG** electrodes (see Figures S15 and S16 in the Supporting Information for spectra). **Table 1** provides the lithium-ion diffusivity (D_{Li+}) and the charge transfer resistance (R_{CT}) of the thin (5 μm, 0.3 mg cm^{-2}) **PNDI-T2** and **PNDI-T2EG** electrodes, which were determined from the EIS measurements.

At 60 wt% polymer content, the D_{Li+} is comparable between the two polymers: 2.97×10^{-12} and 2.65×10^{-12} cm^2 s^{-1} for the **PNDI-T2** and **PNDI-T2EG** electrodes, respectively. However, as we reduced the amount of conductive carbon, the difference increased. With 80 wt% polymer in the electrode, the D_{Li+} of the **PNDI-T2EG** electrodes almost tripled

to 7.01×10^{-12} cm^2 s^{-1}, much higher than that of the 80 wt% **PNDI-T2** electrodes (3.96×10^{-12} cm^2 s^{-1}). This indicates that the D_{Li+} is strongly correlated with rate performance. Both polymers at 60 wt% polymer content showed similar capacity retention, whereas at 80 wt% polymer content the **PNDI-T2EG** electrodes significantly outperformed the **PNDI-T2** electrodes.

Results from EIS measurements also showed significantly reduced R_{CT} for all the **PNDI-T2EG** electrodes tested. The R_{CT} represents the resistance for electron transfer during a redox reaction and can be interpreted as a measure of reactivity at a given discharge state. The **PNDI-T2** electrodes exhibited an order of magnitude higher R_{CT} (246 Ω) than the **PNDI-T2EG** electrodes (45 Ω). With increasing polymer content, an increase in R_{CT} was observed for both electrodes, as expected due to the reduced quantity of conductive carbon. However, the increase in R_{CT} was much larger for the **PNDI-T2** electrodes compared with the **PNDI-T2EG** electrodes. With increasing polymer content from 60 to 80 wt%, R_{CT} increased to 200 and 45 Ω for the **PNDI-T2** and **PNDI-T2EG** electrodes, respectively. Further increasing the polymer content to 100 wt% resulted in R_{CT} values of 1273 and 101 Ω for the **PNDI-T2** and **PNDI-T2EG** electrodes, respectively.

The improvement of the D_{Li+} associated with the reduction of the R_{CT} implies that the EG side chains simultaneously affect both ion and electron transport in the **PNDI-T2EG** electrodes. More information on the redox mechanism of the polymer electrodes was obtained from cyclic voltammetry (CV) measurements as shown in **Figure 3**a. These measurements revealed reversible oxidation processes for both **PNDI-T2** and **PNDI-T2EG** electrodes. However, compared with the **PNDI-T2** electrodes that exhibited sharp redox peaks, **PNDI-T2EG** electrodes exhibited broadened redox peaks with clear shoulders. Furthermore, the reduction potential onset of the **PNDI-T2EG** electrodes (2.8 V) was higher than that of the **PNDI-T2** electrodes (2.5 V), suggesting a lower barrier to electron transport.[42,47] While the source of this broadening and change in potential is unclear, we attribute this to the improved solubility of lithium ions in **PNDI-T2EG** due to the presence of the polar EG side chains. Similar results have been observed in other studies of conjugated polymers with polar side chains.[35,48–50] This is also consistent with improved electronic conductivity and improved rate performance of **PNDI-T2EG** polymer (see Figure 2b,d). The redox mechanism for **PNDI-T2** has been studied extensively and involves a reversible two-step electrochemical reaction with the aromatic imide group.[42,47] Based on the CV measurements, we expect a similar redox mechanism for **PNDI-T2EG** with the addition that the electronic conductivity was highly affected by the ionic conductivity of the electrodes (see Figure 2f).

Table 1. Lithium-ion diffusivities (D_{Li+}) and charge transfer resistances (R_{CT}) from the EIS measurements of the thin **PNDI-T2** and **PNDI-T2EG** electrodes with varying polymer contents.

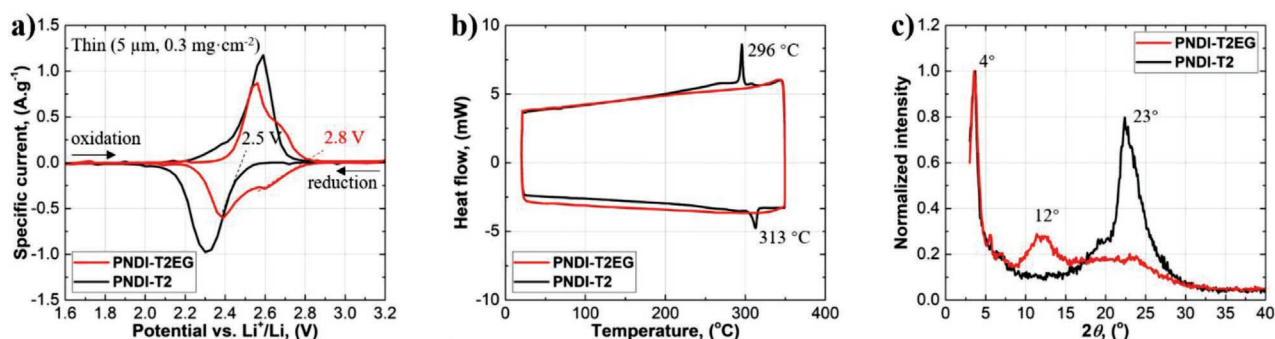|	PNDI-T2			PNDI-T2EG		
Polymer content	60%	80%	100%	60%	80%	100%
D_{Li+} [cm^2 s^{-1}]	2.97×10^{-12}	3.96×10^{-12}	–	2.65×10^{-12}	7.01×10^{-12}	–
R_{CT} [Ω]	114	200	1273	21	45	101

Figure 3. a) CV results for the thin **PNDI-T2EG** and **PNDI-T2** electrodes. b) DSC and c) XRD results for **PNDI-T2EG** and **PNDI-T2**.

Differential scanning calorimetry (DSC) and X-ray diffraction (XRD) measurements provided additional insights into the microstructure of **PNDI-T2** and **PNDI-T2EG**. As shown in Figure 3b, **PNDI-T2** is a highly crystalline material as reflected by sharp melting and crystallizing transitions at 313 and 296 °C, respectively. **PNDI-T2EG** is amorphous and no discernible transitions were observed. In Figure 3c, **PNDI-T2** exhibited sharp diffraction peaks at $2\theta = 4°$ and 23°, representing polymer interchain lamellar stacking and π-stacking.[51,52] **PNDI-T2EG** only exhibited lamellar stacking with very weak π-stacking. While crystallinity is generally favorable for charge transport, **PNDI-T2EG** exhibits higher electronic conductivities compared with **PNDI-T2** despite being an amorphous polymer. This points to the impact of the side chains on electrochemical doping of the conjugated polymer backbone, which serves to significantly increase the conductivity of **PNDI-T2EG**.

The **PNDI-T2EG** nanocomposite electrodes outperformed most previously reported organic electrodes both in terms of performance at high cycling rates, high mass loadings, and high polymer content (see Table S7 in the Supporting Information for detailed comparison). A very few studies for organic electrodes have explored nanocomposite electrodes with mass loadings exceeding 1 mg cm², C-rates above 10C or even 100C, and polymer content over 80 wt% or even up to 100 wt%, which are practical conditions for battery applications, and none exhibited the excellent rate performance observed for the **PNDI-T2EG** electrodes. Although **PNDI-T2EG** exhibited a lower (5–7 times lower) specific capacity than the reported organic electrode materials, the fast or even ultrafast rechargeability makes the **PNDI-T2EG** electrode capable of being charged much faster (10 or 100 times faster) than other organic electrodes, which compensates for the low capacity.

To further quantify the rate performance of **PNDI-T2EG** and compare it to other materials reported in the literature,

we relied on a recently reported semiempirical equation to calculate transport coefficient (Θ), which is used as a figure of merit to describe the rate performance of **PNDI-T2EG** (see Equations (S1) and (S2) in the Supporting Information for calculation details).[53] Results in **Table 2** demonstrate that **PNDI-T2EG** exhibits Θ with an order of magnitude higher than **PNDI-T2**. As shown in **Figure 4**, the highest Θ is 1.4×10^{-10} m² s⁻¹ for the **PNDI-T2EG** nanocomposite electrode with 60 wt% polymer at a mass loading of 1.28 mg cm⁻², which is close to the theoretical rate limit (3×10^{-10} m² s⁻¹).[53] This suggests that **PNDI-T2EG** is among the best electrode materials in terms of rate performance.

3. Conclusions

In summary, we demonstrated that modification of conjugated polymer side chains had a significant impact on the electrochemical performance of nanocomposite electrodes, enabling excellent performance at high charge–discharge rates. For thick electrodes (20 µm, 1.28 mg cm², and an ultrafast charge–discharge rate of 100C (72 s per cycle), the **PNDI-T2EG** electrodes retained an unprecedented 66% of the theoretical specific capacity. Furthermore, **PNDI-T2EG** showed excellent performance even when the polymer content was increased to 80 wt% and had theoretical specific capacity retentions of 68% at 10C (12 min per cycle) and 55% at 100C (72 s per cycle). Additive-free electrodes comprised of **PNDI-T2EG** were also achieved with electrochemical performance up to 20C (6 min per cycle). The presence of the EG side chains improved both lithium-ion diffusivity and the electronic conductivity, resulting in the observed improvement in redox kinetics. This work demonstrates a promising conjugated polymeric material for energy storage in **PNDI-T2EG** and provides a general strategy for improving the performance of conjugated polymer-based electrodes. Other

Table 2. Transport coefficients (Θ) of the **PNDI-T2** and **PNDI-T2EG** electrodes with different mass loadings and polymer contents.

	PNDI-T2	PNDI-T2EG	PNDI-T2	PNDI-T2EG	PNDI-T2	PNDI-T2EG
Mass loading [mg cm⁻²]	0.32	0.32	1.28	1.28	0.32	0.32
Polymer content	60%	60%	60%	60%	80%	80%
Θ [m² s]	9.9×10^{-12}	2.3×10^{-11}	2.6×10^{-11}	1.4×10^{-10}	2.4×10^{-12}	1.2×10^{-11}

**ADVANCED
SCIENCE NEWS**

www.advancedsciencenews.com

**ADVANCED
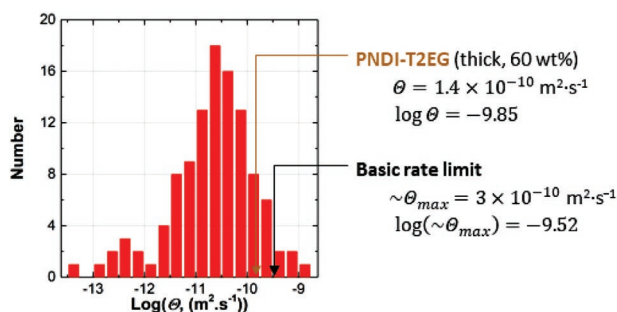FUNCTIONAL
MATERIALS**

www.afm-journal.de

Figure 4. Comparison of transport coefficient (Θ) between **PNDI-T2EG** and other energy storage materials. Adapted with permission.[53] Copyright 2019, Nature Research.

promising polymer-based electrode materials can similarly be modified to potentially increase lithium-ion diffusivity, improve rate capacity, and improve overall capacity. Current studies are focused on understanding how systematic variation of the EG content of the PNDI materials impacts electrochemical performance.

Supporting Information

Supporting Information is available from the Wiley Online Library or from the author.

Conflict of Interest

The authors declare no conflict of interest.

[1] L. Nyholm, G. Nystrom, A. Mihranyan, M. Stromme, *Adv. Mater.* **2011**, *23*, 3751.
[2] M. M. Thackeray, P. J. Johnson, L. A. d. Picciotto, P. G. Bruce, J. B. Goodenough, *Mater. Res. Bull.* **1984**, *19*, 179.
[3] K. Mizushima, P. C. Jones, P. J. Wiseman, J. B. Goodenough, *Mater. Res. Bull.* **1980**, *15*, 783.
[4] M. A. Morris, H. An, J. L. Lutkenhaus, I. Thomas, H. Epps, *ACS Energy Lett.* **2017**, *2*, 1919.
[5] S. Lee, G. Kwon, K. Ku, K. Yoon, S. K. Jung, H. D. Lim, K. Kang, *Adv. Mater.* **2018**, *30*, 1704682.
[6] Y. Liang, Z. Tao, J. Chen, *Adv. Funct. Mater.* **2012**, *2*, 742.
[7] T. B. Schon, B. T. McAllister, P. F. Li, D. S. Seferos, *Chem. Soc. Rev.* **2016**, *45*, 6345.
[8] M. Endo, C. Kim, T. Hiraoka, T. Karaki, M. J. Matthews, S. D. M. Brown, M. S. Dresselhaus, *Mol. Cryst. Liq. Cryst. Sci. Technol., Sect. A* **1998**, *310*, 353.
[9] L. M. Zhu, A. W. Lei, Y. L. Cao, X. P. Ai, H. X. Yang, *Chem. Commun.* **2013**, *49*, 567.
[10] L. W. Shacklette, J. E. Toth, N. S. Murthy, R. H. Baughman, *J. Electrochem. Soc.* **1985**, *132*, 1529.
[11] A. G. MacDiarmid, L. S. Yang, W. S. Huang, B. D. Humphrey, *Synth. Met.* **1987**, *18*, 393.
[12] M. Zhou, J. Qian, X. Ai, H. Yang, *Adv. Mater.* **2011**, *23*, 4913.
[13] N. Gospodinova, L. Terlemezyan, *Prog. Polym. Sci.* **1998**, *23*, 1443.
[14] M. Liu, S. J. Visco, L. C. D. Jonghe, *J. Electrochem. Soc.* **1991**, *138*, 1891.
[15] K. Naoi, K. i. Kawase, M. Mori, M. Komiyama, *J. Electrochem. Soc.* **1997**, *144*, L173.
[16] S.-R. Deng, L.-B. Kong, G.-Q. Hu, T. Wu, D. Li, Y.-H. Zhou, Z.-Y. Li, *Electrochim. Acta* **2006**, *51*, 2589.
[17] T. Suga, H. Konishi, H. Nishide, *Chem. Commun.* **2007**, 1730.
[18] K. Koshika, N. Chikushi, N. Sano, K. Oyaizu, H. Nishide, *Green Chem.* **2010**, *12*, 1573.
[19] K. Oyaizu, T. Suga, K. Yoshimura, H. Nishide, *Macromolecules* **2008**, *41*, 6646.
[20] T. Boschi, R. Pappa, G. Pistoia, M. Tocci, *J. Electroanal. Chem. Interfacial Electrochem.* **1984**, *176*, 235.
[21] Y. Liang, Z. Chen, Y. Jing, Y. Rong, A. Facchetti, Y. Yao, *J. Am. Chem. Soc.* **2015**, *137*, 4956.
[22] H. Dong, Y. Liang, O. Tutusaus, R. Mohtadi, Y. Zhang, F. Hao, Y. Yao, *Joule* **2019**, *3*, 782.
[23] Z. Song, H. Zhan, Y. Zhou, *Chem. Commun.* **2009**, *448*, 448.
[24] B. D. Paulsen, K. Tybrandt, E. Stavrinidou, J. Rivnay, *Nat. Mater.* **2020**, *19*, 13.
[25] J. Chung, A. Khot, B. M. Savoie, B. W. Boudouris, *ACS Macro Lett.* **2020**, *9*, 646.
[26] R. Kroon, D. Kiefer, D. Stegerer, L. Yu, M. Sommer, C. Muller, *Adv. Mater.* **2017**, *29*, 1700930.
[27] J. Li, C. W. Rochester, I. E. Jacobs, E. W. Aasen, S. Friedrich, P. Stroeve, A. J. Moulé, *Org. Electron.* **2016**, *33*, 23.
[28] D. Kiefer, A. Giovannitti, H. Sun, T. Biskup, A. Hofmann, M. Koopmans, C. Cendra, S. Weber, L. J. Anton Koster, E. Olsson, J. Rivnay, S. Fabiano, I. McCulloch, C. Muller, *ACS Energy Lett.* **2018**, *3*, 278.
[29] J. Liu, L. Qiu, G. Portale, M. Koopmans, G. Ten Brink, J. C. Hummelen, L. J. A. Koster, *Adv. Mater.* **2017**, *29*, 1701641.
[30] A. Giovannitti, C. B. Nielsen, D. T. Sbircea, S. Inal, M. Donahue, M. R. Niazi, D. A. Hanifi, A. Amassian, G. G. Malliaras, J. Rivnay, I. McCulloch, *Nat. Commun.* **2016**, *7*, 13066.
[31] A. Giovannitti, K. J. Thorley, C. B. Nielsen, J. Li, M. J. Donahue, G. G. Malliaras, J. Rivnay, I. McCulloch, *Adv. Funct. Mater.* **2018**, *28*, 1706325.
[32] L. R. Savagian, A. M. Osterholm, J. F. Ponder, Jr., K. J. Barth, J. Rivnay, J. R. Reynolds, *Adv. Mater.* **2018**, *30*, 1804647.
[33] G. S. Collier, I. Pelse, J. R. Reynolds, *ACS Macro Lett.* **2018**, *7*, 1208.
[34] A. Giovannitti, I. P. Maria, D. Hanifi, M. J. Donahue, D. Bryant, K. J. Barth, B. E. Makdah, A. Savva, D. Moia, M. Zetek, P. R. F. Barnes, O. G. Reid, S. Inal, G. Rumbles, G. G. Malliaras, J. Nelson, J. Rivnay, I. McCulloch, *Chem. Mater.* **2018**, *30*, 2945.
[35] P. A. Finn, I. E. Jacobs, J. Armitage, R. Wu, B. D. Paulsen, M. Freeley, M. Palma, J. Rivnay, H. Sirringhaus, C. B. Nielsen, *J. Mater. Chem. C* **2020**, *8*, 16216.
[36] M. A. Ratner, D. F. Shriver, *Chem. Rev.* **1988**, *88*, 109.
[37] P. V. Wright, *J. Polym. Sci., Polym. Phys. Ed.* **1976**, *14*, 955.
[38] W. Yan, C. Wang, J. Tian, G. Zhu, L. Ma, Y. Wang, R. Chen, Y. Hu, L. Wang, T. Chen, J. Ma, Z. Jin, *Nat. Commun.* **2019**, *10*, 2513.
[39] Y. Zu, Y. Xu, L. Ma, Q. Kang, H. Yao, J. Hou, *ACS Appl. Mater. Interfaces* **2020**, *12*, 18457.

[40] Y. Wang, Z. Liu, C. Wang, Y. Hua, H. Lin, W. Kong, J. Ma, Z. Jin, *Energy Storage Mater.* **2020**, *26*, 494.

[41] M. R. Raj, R. V. Mangalaraja, G. Lee, D. Contreras, K. Zaghib, M. V. Reddy, *ACS Appl. Energy Mater.* **2020**, *3*, 6511.

[42] Y. Liang, P. Zhang, J. Chen, *Chem. Sci.* **2013**, *4*, 1330.

[43] H. H. Rehan, *J. Power Sources* **2003**, *113*, 57.

[44] A. Mirmohseni, R. Solhjo, *Eur. Polym. J.* **2003**, *39*, 219.

[45] H. Olsson, E. J. Berg, M. Strømme, M. Sjödin, *Electrochem. Commun.* **2015**, *50*, 43.

[46] M. E. Bhosale, S. Chae, J. M. Kim, J.-Y. Choi, *J. Mater. Chem. A* **2018**, *6*, 19885.

[47] Z. Song, H. Zhan, Y. Zhou, *Angew. Chem., Int. Ed.* **2010**, *49*, 8444.

[48] M. Matta, R. Wu, B. D. Paulsen, A. J. P.II, R. Sheelamanthula, I. McCulloch, G. C. Schatz, J. Rivnay, *Chem. Mater.* **2020**, *32*, 7301.

[49] Z. S. Parr, R. Halaksa, P. A. Finn, R. B. Rashid, A. Kovalenko, M. Weiter, J. Rivnay, J. Krajcovic, C. B. Nielsen, *ChemPlusChem* **2019**, *84*, 1384.

[50] A. I. Hofmann, R. Kroon, L. Yu, C. Muller, *J. Mater. Chem. C* **2018**, *6*, 6905.

[51] Y. Guo, W. Sato, K. Inoue, W. Zhang, G. Yu, E. Nakamura, *J. Mater. Chem. A* **2016**, *4*, 18852.

[52] M. M. Durban, P. D. Kazarinoff, C. K. Luscombe, *Macromolecules* **2010**, *43*, 6348.

[53] R. Tian, S. H. Park, P. J. King, G. Cunningham, J. Coelho, V. Nicolosi, J. N. Coleman, *Nat. Commun.* **2019**, *10*, 1933.